Proceedings of the Institute of Acoustics

ROOM ACOUSTICS MODELLING USING DIGITAL WAVEGUIDE MESH STRUCTURES

Damian T. Murphy Department of Electronics, University of York, Heslington, York, YO10 5DD
David M. Howard Department of Electronics, University of York, Heslington, York, YO10 5DD

1. INTRODUCTION

Generic filter plus delay-line based reverberation algorithms have proved highly effective at modelling the characteristics of an acoustic space [1] although when modelling a particular space or environment a more detailed approach is required. The acoustic properties of a real enclosed space based on its geometrical and physical properties can be uniquely defined by measuring the Room Impulse Response (RIR) at a specific listening point for an input signal applied at a given sound source location. Geometrical acoustic methods are typically used to tackle this problem although digital waveguide mesh structures provide an alternative accurate and efficient method of modelling the properties of many resonant objects, including acoustic spaces. 2-D rectilinear and triangular mesh structures have been used extensively in the past to model plates and membranes [2] and are presented here as potential analogues to 2-D acoustic spaces. This paper examines how mesh structures are constructed so that Room Impulse Responses (RIRs) can be obtained for a distinct point. Measuring over a number of points results in 5.1 channel RIRs suitable for surround sound reverberation processing. Wave propagation is observed, RIR measurements are taken and comparisons are made regarding the spectral content and the associated properties when compared with standard room acoustics parameters. The limitations of such models are discussed and possibilities for enhanced mesh structures are suggested.

2. GEOMETRICAL ACOUSTICS - AN OVERVIEW

Geometric acoustic models treat sound waves as a ray allowing the path of a propagating wave to be examined with considerable clarity and rigour. Specular reflections at a surface can be considered where the angle of incidence is equal to the angle of reflection. Absorption can also be accounted for where the ray loses a percentage of its energy in a frequency dependent manner according to the absorption coefficient of the reflecting surface in question. Absorption due to the propagating medium proportional to the distance travelled by the sound ray can also be modelled. Geometric models are based on the assumption that the surfaces involved are essentially flat and large compared to the wavelength of sound being considered. This implies that these models are only valid for high frequencies and larger spaces. They are further limited as they do not in general take account of other wave phenomena. Diffraction effects cannot be accounted for as propagation in straight lines is an inherent part of the model. Similarly, interference effects are disregarded as there are no phase components to superimposed rays, as is diffusion due to all reflections being considered as specular. Therefore in the low frequency regions where these effects are particularly noticeable and in spaces where the physical dimensions are comparable to the wavelength of the sound source being investigated, the ray approach becomes invalid.

2.1 THE RAY-TRACING METHOD

Ray-tracing was first applied to concert hall acoustics by Krokstad, Strøm, and Sørsdal in 1968 and was essentially the first attempt to arrive at a digitally modelled RIR [3]. A sound source is imagined

to release a number of sound rays in all directions at a certain moment in time. The path of each ray, taking into account all reflections at walls or objects, is followed, and when it arrives at a previously designated point, its energy, arrival time, direction and any other relevant information is calculated and recorded. This can be plotted as a histogram showing the temporal distribution of the energy received, and can be seen as an approximation to the impulse response of the acoustic space, determined by the number of particle paths calculated, and the time resolution achieved.

There are a number of limitations associated with ray tracing techniques. The size of the detector has to be considered, as it is not possible to model it as a point. An infinitely small detector cannot detect an infinitely small sound ray although variable size detectors dependent on the number of rays and their individual length can be used to improve detection accuracy. In simple rooms the number of rays required for accuracy is not too high. However, as reflection orders and the complexity of the room geometry increase then the number of rays required increases by a significant amount. Due to the angle between adjacent rays emitted from the point source remaining approximately constant, as the ray length becomes longer, the model becomes less exact. This has been improved upon by using diverging beam techniques such as pyramid and cone tracing [4].

2.2 THE IMAGE-SOURCE METHOD

The Image-Source method [5] is based on the idea that a sound ray reflected from a plane wall can be imagined as originating from an *image source*. This is the mirror image of the original sound source formed by the wall, the wall being the plane of reflection. Clearly the distance via the reflected route is equivalent to the direct line between the image-source and the listener. As there will be more than one wall in an enclosed space, this mirroring process has to be carried out to image sources already constructed, leading to second-order images, third-order images and so on. The final pattern of image sources, which is basically infinite, represents the original acoustic space. Rather than having to trace the individual ray paths, the contributions of all the individual image sources taking into account the $1/r^2$ law, wall absorption and air attenuation are merely added together. For a given source/listener combination each source will emit only one ray in a direction defined by the point where the listener is located. This is clearly an improvement over ray-tracing methods as there is no need to consider ray emission directions or detector size and shape.

This process is relatively straightforward for simple rectangular shaped rooms, although rapidly becomes non-trivial for more complex geometries. Even for rectangular rooms the number of image sources increases exponentially with the number of reflections, giving an associated rise in computation time. With more complex spaces there is a further rise in computation time associated with the need to perform visibility checks on each image-source as not all of the image-sources created due to the planes of reflection constructed by the room's geometry can physically exist.

3. 2-D DIGITAL WAVEGUIDE MESH STRUCTURES

A waveguide is any medium in which wave motion can be characterised by the one-dimensional wave equation. In the lossless case, all solutions can be expressed in terms of left-going and right-going travelling waves and can be simulated using a bi-directional digital delay line. A digital waveguide model is obtained by sampling, both in space and time, the one-directional travelling waves occuring in a system of ideal lossless waveguides [6]. The sampling points in this case are called scattering junctions, and are connected by bi-directional unit-delay digital waveguides. Figure 1 shows the general case of a scattering junction J with N neighbours, $i = 1,2,\ldots N$.

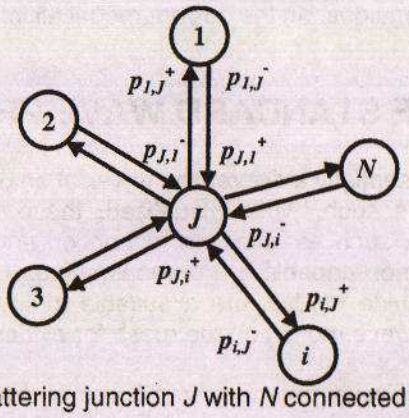

Figure 1: A general scattering junction J with N connected waveguides for $i = 1,2,\ldots,N$.

The sound pressure in a waveguide is represented by p_i, the volume velocity by v_i and the impedance of the waveguide by Z_i. The input to a waveguide is termed p_i^+ and the output p_i^-. The signal $p_{i,J}^+$ therefore represents the incoming signal to junction i along the waveguide from the opposite junction J. Similarly, the signal $p_{i,J}^-$ represents the outgoing signal from junction i along the waveguide to the opposite junction J. The volume velocity v_i is equal to pressure, p_i, divided by impedance, Z_i. The delay elements are bi-directional and so the sound pressure is defined as the sum of its input and output:

$$p_i = p_i^+ + p_i^- \qquad (1)$$

At a lossless scattering junction with N connected waveguides the following conditions must hold:

1. The sum of the input volume velocities, v^+, equals the sum of the output volume velocites, v^-:

$$\sum_{i=1}^{N} v_i^+ = \sum_{i=1}^{N} v_i^- \qquad (2)$$

2. The sound pressures in all crossing waveguides are equal at the junction:

$$p_1 = p_2 = \ldots = p_i = \ldots = p_N \qquad (3)$$

Using these conditions the sound pressure at a scattering junction can be expressed as:

$$p_J = \frac{2\sum_{i=1}^{N} \frac{p_i^+}{Z_i}}{\sum_{i=1}^{N} \frac{1}{Z_i}} \qquad (4)$$

As the waveguides are equivalent to bi-directional unit-delay lines, the input to a scattering junction is equal to the output from a neighbouring junction into the connecting waveguide at the previous time step. This can be expressed as:

$$p_{J,i}^+ = z^{-1} p_{i,J}^- \qquad (5)$$

To model the propagation of a wave on the horizontal plane within an enclosed space, 2-D rectilinear and triangular mesh structures can be constructed using unit delay waveguides and lossless scattering junctions with $N = 4$ and $N = 6$ in Equation 4 respectively. A signal representing

acoustic pressure introduced to a waveguide will propagate in either direction along the bi-directional delay lines until it comes to a junction. The signal then scatters according to the relative impedances of the connected waveguides. In the current model all impedances are set to be equal.

4. OBSERVATION OF STANDARD WAVE PHENOMENA

Waveguide mesh structures are essentially a discretized physical analogue of a continuous medium supporting wave propagation. As such, when visualised, these mesh models should exhibit standard typical wave phenomena, such as reflection, diffraction and interference, properties that geometric acoustic models are not capable of demonstrating. Therefore the first step in establishing whether these waveguide models are a suitable alternative to geometrical acoustic models is to examine the resulting wave motion on the mesh for evidence of these phenomena.

Figure 2 shows a plan view of the wavefronts on a rectilinear and triangular mesh 14 time steps after each has been excited with a Gaussian impulse applied over 6 time steps.

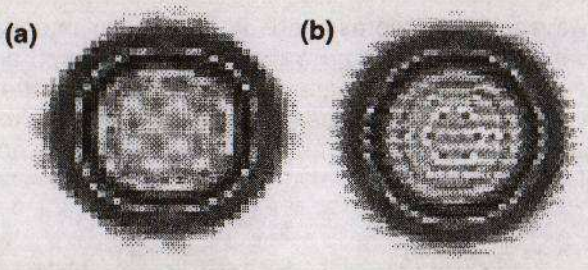

Figure 2: Wavefronts on, (a) rectilinear mesh, and (b) triangular mesh, 14 time steps after an applied Gaussian impulse.

In Figure 2(a) the circular wavefront is clearly non-uniform, with "fuzzy" edges on the top, bottom and sides. This is due to the direction dependent dispersion error present on the rectilinear mesh. An inherent problem with lattice type structures such as the digital waveguide mesh is that they exhibit frequency and angular dependent dispersion, whereas in the ideal case all wave frequencies travel at the same speed in every direction. This property is dependent upon the mesh topology as well as the mesh density. The wavefront along the diagonals to the mesh (if it were to be super-imposed on top of this image) are actually quite sharp and defined. It can be shown mathematically [6] that there is no dispersion on the rectilinear mesh along the diagonals to the mesh coordinate system. However the top, bottom and sides of the wavefront are not so well defined due to the dispersion error being maximum in these directions. The wavefront on the triangular mesh, however, is much closer to being a uniform circle.

One of the most significant benefits in using a waveguide mesh in modelling the acoustics of a room is that reflection, diffraction and interference effects are a natural consequence of the resulting wave propagation. An example is shown in Figure 3 where a rectilinear mesh models a rectangular room with a dividing wall partitioning it into two coupled spaces. This dividing wall has gaps placed in it and when an impulse is applied in one half of the room, the wave propagates through the gaps in the wall and proceeds to spread out into the other half of the room. The curved edge of the resulting re-constructed wavefront gives a clear example of diffraction and constructive interference as the three individual waves unite in a single wavefront.

Further examples of wave phenomena are shown in Figure 4. Diffraction of sound due to an object being placed in a room is shown in Figure 4(a). The reflected wave, labelled (A) and the diffracted wave, labelled (B), are clearly apparent, with the latter about to reform as a single unified wavefront.

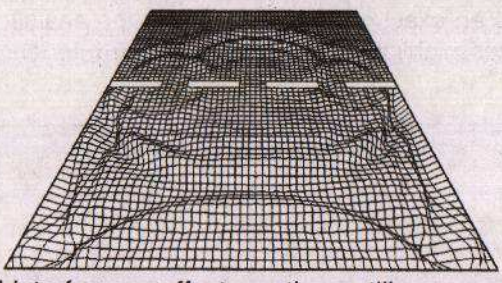

Figure 3: Diffraction and interference effects on the rectilinear mesh due to the gaps in the dividing wall placed into this model of a rectangular room.

An example of interference sometimes found in geometrical room designs where one end of the space is approximately semi-circular or concave can also be demonstrated. This can result in an uneven distribution of modes and sound pressure level due to the focusing properties of the shape of the room as shown in Figure 4(b). The three reflections from the angled walls at the upper concave end of the room converge constructively at the focal point **(F)**. Increased absorption at these walls would help to alleviate this problem as would diffusers, as they would help to scatter the sound waves over a wider area avoiding the convergence at **(F)**.

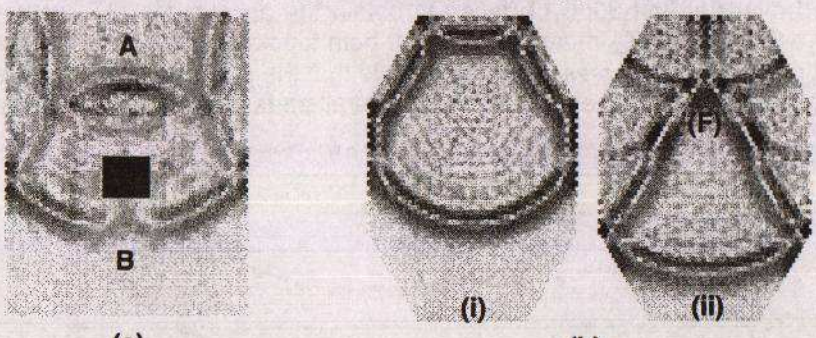

Figure 4: (a) Diffraction and reflection due to an object being placed in the room. (A) Reflected wave; (B) Diffracted wave; (b) A room with slightly concave ends. (i) The reflections from the three angled walls at the upper end of the room start to converge; (ii) the result is a focal point marked (F) giving an uneven distribution of sound pressure level.

5. RIR MEASUREMENT AND ANALYSIS

A number of RIR measurements for both triangular and rectilinear mesh topologies were made for a 2-D representation of a rectangular room, 7.0m long and 6.0m wide, with a fixed source, four different output points, and varied boundary absorption conditions. To generate a satisfactory audio rate RIR, a mesh sampling rate of at least 44.1kHz is required. The sampling rate of the mesh is determined by, $f_{update} = c\sqrt{2}/d$ where d is the distance between junctions and c is the speed of sound. With $c = 343\ ms^{-1}$ and $d = 0.011m$, f_{update} = 44098Hz. A 2-second Room Impulse Response (RIR) measurement was made in each case.

Figure 5 shows a measured RIR in the frequency domain for the triangular mesh topology up to the approximate critical frequency of the room, below which modal behaviour is dominant. All walls are set to be totally reflecting with no absorption, the RIR has the first 0.2s removed to eliminate any transient response and the remaining 1.8s has an FFT applied to it using a Kaiser-Bessel window. For comparison, the analytical room modes have been calculated and plotted on the same graph. In these cases only axial (reflections between two surfaces denoted by the longer dashed lines) and

tangential (reflections between four surfaces denoted by the shorter dashed lines) are valid. It can clearly be seen that there is an exact correlation between the analytical room modes as calculated and the resonant frequencies highlighted by examining the frequency response of the measured RIR.

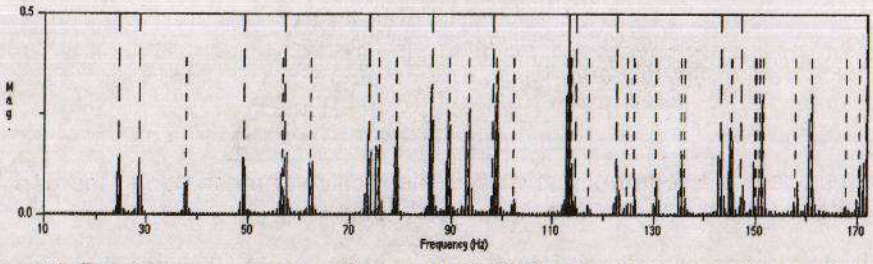

Figure 5: Frequency response of room modelled using the triangular mesh below the approximate critical frequency. Analytical axial modes are shown as long dashed lines. Analytical tangential modes are shown as shorter dashed black lines.

Reverberation Time measurements are obtained according to ISO3382 [7]. The RIR is octave-band filtered, squared to obtain the acoustic energy and backward-integrated, with a linear regression being performed over the first 30dB of decay to obtain the appropriate RT_{60} values. It can been seen from Figure 6 that the RT_{60} measurements for both topologies are generally consistent across all of the output points. This agrees with the principle that the reverberant sound present in a room should be diffuse – that is, the reverberant sound visits all parts of the room with equal probability.

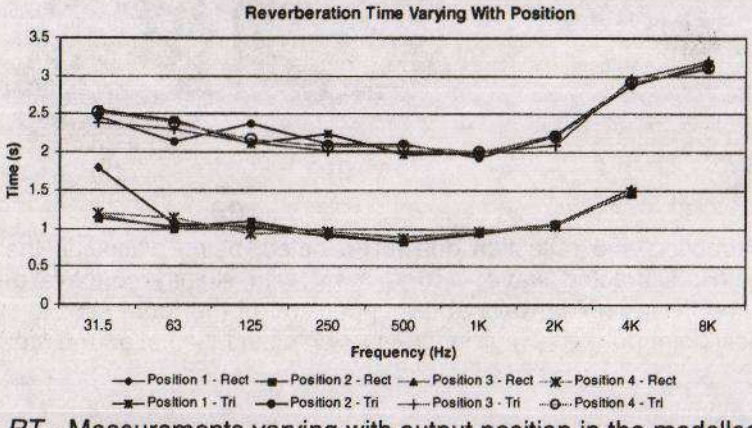

Figure 6: RT_{60} Measurements varying with output position in the modelled room, for both the triangular mesh (upper set of plots) and the rectilinear mesh (lower set of plots).

Note that the RT_{60} values for the triangular mesh are approximately double those of the rectilinear mesh. When a Dirac impulse is applied as an input to the rectilinear mesh, every other sample value is equal to zero in the resultant RIR. This is because the path length of every route between two arbitrary junctions is either an odd or even number of waveguide elements, each being a unit delay. Therefore in the rectilinear mesh there does not exist a pair of junctions which can be reached by both an odd and even number of unit waveguide elements. Conversely in the triangular waveguide mesh, there exists both an odd and even length path between any two junctions. Given that the RIRs from the rectilinear mesh have every other sample value equal to zero it is clear that there is a much lower average signal strength and hence less reverberant energy present. RIRs from the triangular mesh have double the number of non-zero samples and hence the RT_{60} measurements are correspondingly longer – approximately twice as long as those from the rectilinear mesh.

6. SURROUND-SOUND REVERBERATION RIRS

It is generally given that for a high quality reverberation effect with a sense of depth and envelopment suitable for surround sound applications, the reverberant signals at each surround output should be fully decorrelated [8]. To test the suitability of this modelling technique for obtaining surround sound RIRs a rectangular room 8.0m long and 5.0m wide has been modelled using the triangular mesh. The sound source input is situated in the top left corner, 1.0m from each wall. A 5.1 surround-sound RIR is measured around a point situated 6.0m from the top wall and 2.5m from the left wall as shown in Figure 7. Each of the 5.1 RIR measurements has an omnidirectional characteristic with each measuring position being located on the circumference of a circle 1.0m radius from the centre point.

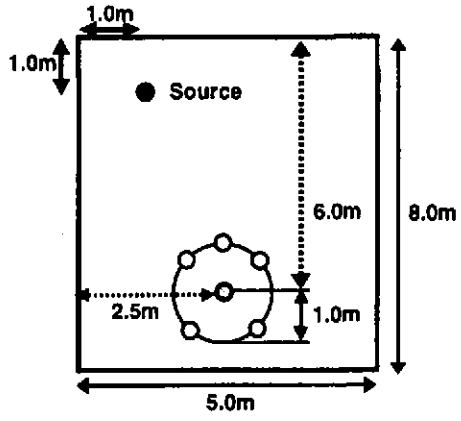

Figure 7: Plan view of the modelled room showing positions of input sound source and 5.1 RIR measurement points based around a central output position.

Despite the simple geometrical layout of the room, with uniform absorption/reflection conditions along each boundary, there is evidence of significant decorrelation in the RIRs. Figure 8(b) shows the normalised cross-correlation between the Centre and Right Surround RIRs, which is typical for the cross-correlation of any pair of RIRs obtained. Clearly this is an encouraging result showing that this technique is appropriate for surround sound reverberation modelling. By way of comparison Figure 8(c) shows the normalised cross-correlation between the left and right channels of a generic "good quality" filter based reverberation algorithm, showing that the correlation between outputs in this case is even less.

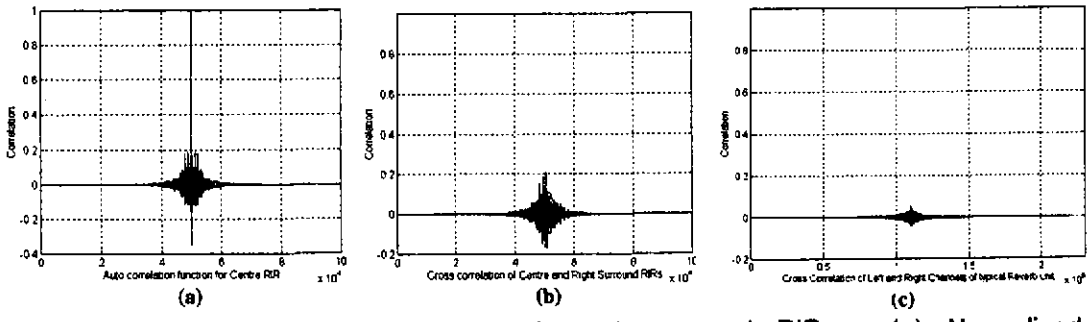

Figure 8: Cross-correlation functions for 5.1 surround RIRs. (a) Normalised autocorrelation function for Centre RIR; (b) Normalised cross-correlation function for the Centre and Right RIRs; (c) Normalised cross-correlation function for the left and right channels of a typical filter based reverberator.

7. CONCLUSIONS

This paper has introduced and examined how digital waveguide mesh models provide an alternative to geometric methods for modelling the acoustics of a room. Results show that this is a promising technique, demonstrating the characteristics of natural wave motion, accurate detection of modal frequencies, and appropriate reverberation characteristics. Further with surround sound applications becoming more commonplace this model incorporates the property of naturally decorrelated reverberation when multi-channel output RIRs are obtained.

Work is ongoing to overcome the limitations of the technique so that a better quality reverberation effect can be obtained. The triangular mesh is the most favourable mesh topology as it minimises dispersion error effects due to the direction of wave propagation in the 2-D plane [9]. Pre and post processing using frequency warping techniques can help to correct spectral errors due to frequency dependent dispersion [10], allowing smaller resolution mesh structures to be used for a given geometry for a required bandwidth. Oversampling the modelled space using high-resolution mesh structures also results in improved RIR measurements although at the expense of increased computation time [9]. The use of 3-D tetrahedral mesh structures can provide a full 3-D room model [11], but again with the result being increased computation time, an increase in the complexity of the structure and related 3-D dispersion error characteristics. Further developments will include a more detailed analysis of the boundary characteristics and the implementation of frequency dependent boundary conditions, modelling the characteristics of air absorption due to propagation through the mesh and improvements in RIR execution time.

8. REFERENCES

[1] J. A. Moorer, "About this Reverberation Business", *Computer Music Journal*, Vol. 3, No. 2, pp. 13-27, 1979.

[2] Fontana, F., and Rocchesso, D., "A New Formulation of the 2D-Waveguide Mesh for Percussion Instruments", *Proceedings of the XI Colloquium on Musical Informatics*, pp. 27-30, Bologna, Italy, November 1995.

[3] Krokstad A., Strøm S., and Srøsdal, S., "Calculating the Acoustical Room Response by use of a Ray Tracing Technique", *Journal of Sound Vibration*, Vol. 8, No. 1, pp 118-125, 1968.

[4] Farina, A., "Pyramid Tracing Vs Ray Tracing for the simulation of sound propagation in large rooms", *Computational Acoustics and its Environmental Applications*, pp. 109-116, Editor C.A. Brebbia, Computational Mechanics Publications, Southampton (GB) 1995.

[5] Stephenson, U., "Comparison of the Mirror Image Source Method and the Sound Particle Simulation Method", *Applied Acoustics*, Vol. 29, pp 35-72, 1990.

[6] Van Duyne, S. A. and Smith, J. O., "Physical Modeling with the 2-D Digital Waveguide Mesh", *Proceedings of the International Computer Music Conference*, pp. 40-47, Tokyo, Japan, 1993.

[7] International Standard 3382, "Acoustics – Measurement of reverberation time of rooms with reference to other acoustical parameters", ISO, Second Edition, 1997.

[8] Griesinger, D., "The Theory and Practice of Perceptual Modeling – How to use Electronic Reverberation to Add Depth and Envelopment Without Reducing Clarity", *Preprint from the Nov. 2000 Tonmeister Conference*, Hannover, available from http://world.std.com/~griesngr/

[9] D.T. Murphy and D.M. Howard, "2-D Digital Waveguide Mesh Topologies in Room Acoustics Modelling", *Proceedings of the Cost G-6 Conference on Digital Audio Effects (DAFX-00)*, pp 211-216, Verona, Italy, Dec. 7-9, 2000.

[10] Savioja, L., and Välimäki, V., "Reducing the dispersion error in the Digital Waveguide Mesh Using Interpolation and Frequency-Warping techniques", *IEEE Transactions om Speech and Audio Processing*, Vol. 8, No. 2, pp. 184-194, Mar. 2000.

[11] Campos, G., and Howard, D. M., "A Parallel 3-D Digital Waveguide Mesh Model With Tetrahedral Topology for Room Acoustic Simulation", *Proceedings of the COST G-6 Conference on Digital Audio Effects (DAFX-00)*, pp. 73-78, Verona, Italy, Dec. 7-9, 2000.